BioCore
Exploring Scientific Community

International Journal of Nanotechnology in Medicine & Engineering

Research Article
ISSN 2474-8811

# Electrochemical characterization of Metal injection moulded Ti6Al7Nb used for dental applications under varying saliva conditions

**Onoyivwe Monday Ama[*1,3], Khotso Khoele[2,3], Suprakas Sinha Ray[1, 3]**

[1]*Department of Applied Chemistry, University of Johannesburg, Doornfontein, 2028, Johannesburg, South Africa*
[2]*Tshwane University of Technology, Department of Chemical, Metallurgical and Materials Engineering, Pretoria, South-Africa*
[3]*DST-CSIR National Center for Nanostructured Materials, Council for Scientific and Industrial Research, Pretoria 0001, South Africa*

## Abstract

In avoidance of metal ions into the human bloodstream, $Ti_6Al_7Nb$ became a subsequent alloy for various implant's purpose. In this study, different corrosion techniques have been utilized to characterize corrosion behavior of $Ti_6Al_7Nb$ alloy in pure saliva simulating electrolyte (SSE), varying fluoride conditions, and different peroxide concentrations as well as under severe plaque conditions when $Ti_6Al_7Nb$ alloy is used for dental applications. With an exhibition of passivity range within most engaged conditions, Potentiodynamic polarization (PDP) curves generally revealed $Ti_6Al_7Nb$ as good material for dental applications. Nonetheless, the increment of fluoride, peroxide ($H_2O_2$) concentration and severe plaque conditions showed a negative impact on $Ti_6Al_7Nb$ alloy. This observation was clearly observed from electrochemical impedance spectroscopy (EIS) curves as the most compressed semicircles were found under those conditions. A critical fluoride concentration on the surface of the $Ti_6Al_7Nb$ alloy was found to be 5g/l. In attesting to the later, surface morphologies under pure SSE was noble, while it was rapidly degraded under severe plaque condition.

**Keywords:** Corrosion, Ti6Al7Nb, PDP, SSE and EIS

**Corresponding author: Onoyivwe Monday Ama**

Department of Applied Chemistry, University of Johannesburg, Doornfontein, 2028, Johannesburg, South Africa

**Email:** onoyivwe4real@gmail.com

**Citation:** Onoyivwe Monday Ama et al. (2018) Electrochemical characterization of Metal injection moulded $Ti_6Al_7Nb$ used for dental applications under varying saliva conditions. Int J Nano Med & Eng. 3:7, 71 - 77



**Received:** October 05, 2018
**Accepted:** October 15, 2018
**Published:** November 29, 2018

## Introduction

Due to low specific weight, good mechanical properties, low young modulus, very good strain-controlled and notch fatigues resistance, high strength-to-weight-ratio, superior corrosion resistance, etc., titanium (Ti) and its alloys lead on the utilization of biomedical and dental implants [1-4]. The Versatility of Ti and its alloys is from three categories it's normally found from: α, (α+β) and β phases [5, 6]. Within these categories, different problems exist.

$Ti_6Al_4V$ (α+β phases) has a complexity of toxicity elements which release into the body fluid during their applications as implants [7-9].

In particular, aluminium (Al) and vanadium (V) release lead to inflammation and cytotoxicity in the surrounding tissue of implants. In fact, an accumulation of metallic ions in body fluid causes hypersensitivity and thrombogenesis, and these consequent to implant loosening. The worst consequence of ions release into the body entails difficulties such as revision and/or removal of implants [9-12]. In avoidance of toxicity elements release into the blood fluid, $Ti_6Al_7Nb$ has subsequently been developed [13],[14],[15, 16].

Corrosion measurements for pertaining to wimplant usage has previously being done by numerous authors, and different findings have been documented[17],[18],[19],[20]. Furthermore, in consideration of localized corrosion occurrence which goes with non-uniformity pH around implants[21], varying electrolyte conditions have been found to play a critical role on the lifespan of the implant. Fojt et al. [11] utilized corrosion measurements on the characterization of porous Ti39Nb using phosphate-buffered saline solution as an electrolyte. It was found that porosity above certain limit could cause localized corrosion. With an utilization of Ringer solutions at different pH corresponding to severe conditions human body experiences due to surgery, infections and inflammations, Calderon Moreno et al. [22] provided in roads through utilization of electrochemical measurements. Most of all, fluoride which is normally used in toothpaste were found to be problematic at certain concentration [23-25].

Metal injection moulding (MIM) as the state-of-art powder metallurgy manufacturing technique which produces alloys on a mass production of complex small-medium parts has got quite a number of advantages over conventional manufacturing techniques which can be found elsewhere [26] [19, 27]. On the research of the components fabricated by MIM, most authors studied and reported on mechanical properties,

chemical and biocompatibility properties of newly improved materials [26, 28-36]. However, there are no corrosion measurements, particularly, on deeper characterization of passive layer which forms on $Ti_6Al_7Nb$ manufactured by MIM when it's exposed dynamic conditions for dental usage. The present study engaged for corrosion measurements to focus on the empirical occurrence of localised corrosion on $Ti_6Al_7Nb$ manufactured by MIM processes when it is used for dental applications.

## Experimental

**Materials and Solution:** $Ti_6Al_7Nb$ specimens manufactured by MIM were provided in dimensions of $2cm^2$. The Standard electrolyte used in this work was Fusayama-Meyer artificial saliva, and the composition was synthesized from the following chemical powders: NaCl (0.4 g/L), KCl (0.4 g/L) $CaCl_2 . 2H_2O$ (0.796 g L1), $NaH_2$-$PO_4 . 2H_2O$ (0.690 g/L), $Na_2S . 9H_2O$ (0.005 g/L) and Urea (1 g/L). The saliva simulating electrolyte (SSE) was prepared using deionised water with a resistivity of 18.2 MV cm. Certified reagents supplied by Alfa Aesar, USA. NaF (Sigma Aldrich, USA) was added to the artificial saliva solution to simulate different fluoridate media, and it was varied up until a critical concentration was obtained. As based from the literature, for the simulation of the plaque conditions, sulphuric acid ($H_2SO_4$) was used to lower the pH of the pure SSE to 3.0, while the peroxide solutions in SSE (0.1% and 10%) were obtained following steps that can be found elsewhere [37, 38].

**Electrochemical Measurements:** An electrochemical cell with three imperative openings was used in this study to simulate localized corrosion occurrence on bare $Ti_6Al_7Nb$ in the dynamic SSE. Three openings were for engaged electrodes: a working electrode ($Ti_6Al_7Nb$), a platinum wire (counter electrode) and 3M Ag/AgCl as a reference electrode. The whole setup was computerized from advance autolab PGSTAT302 N potentiostat.

Prior to any electrochemical measurement, the OCP was run at room temperature for at least 2 hrs. After OCP measurements, Potentiodynamic polarization (PDP) and Electrochemical impedance spectroscopy (EIS) measurements were carried out. Firstly, the potential of 250 mV was scanned in the reverse direction (cathodically polarized) to remove oxide which formed on the surface of the LCS electrode during an attainment of steady-state conditions under OCP. Secondly, the anodic and cathodic curves were measured at the scan rate of 0.16mV/s; starting from -1 V to 1.5 V.

For EIS measurements, NOVA 2.0.1 software was utilized. The Measurements were carried out at OCP over a frequency scan ranging from 100 kHz to 100 mHz. The wave type was single sine at an integration time of 0.125s per cycle and the amplitude used was 10 mV. Ultimately, after an acquisition of EIS spectra, an electrical equivalent circuit (EEC), which was attained through Boukamp model, was utilized to interpret the EIS data. For reproducibility of the results, all the electrochemical measurements were triplicated.

**Surface Characterization:** Scanning electron microscopy (SEM) coupled to energy-dispersive spectroscopy (EDS) was used to inspect the surface phase morphologies and elemental compositions of the engaged samples. The used SEM was JEOL JSM electron microscope, and it was operated at 20 kV.

## Results and Discussion

Corrosion Measurements results: Fig. 1 below shows the OCP curves for all engaged $Ti_6Al_7Nb$ electrodes in the dynamic SSE used in this study. As can be seen from the Figure, the OCP for 0.1 % $H_2O_2$ is more positive than the other OCPs. This could be due to a momentary oxidization which occurs on the surface of the electrode. In comparison with the higher content (10% $H_2O_2$), an exhibition of more negative CP potential can be seen in Fig. 1. Furthermore, it can also be seen that increasing of the fluoride content and existence of plaque condition led to OCP values shifting from noble values. This could be due to an aggressive effect on the passivation layer of $Ti_6Al_7Nb$ within those electrolyte media [39, 40].

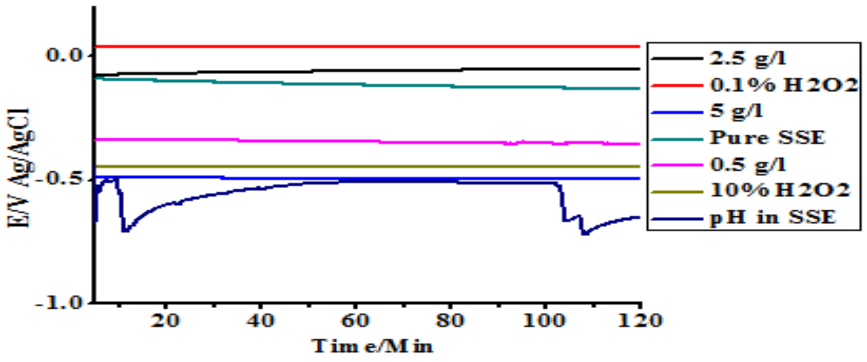


**Fig.1:** OCP curves for $Ti_6Al_7Nb$ in different SSE conditions

On the other hand, Fig. 2 shows PDP curves, and it was intended to characterize the corrosion behavior of $Ti_6Al_7Nb$ in engaged SSE conditions. As can be seen in Fig. 2, $Ti_6Al_7Nb$ shows active-passive behavior as it starts reacting with electrolyte under all engaged conditions. As time goes on, it forms a compact passive layer which prohibits further active transition, particularly under pure SSE. However, with inclusion and increment of fluoride concentration, anodic curves deviate a bit from noble region, and the critical concentration was found to be 2.5 g/l NaF. An initial introduce of peroxide (0.1% H202) shited corrosion potential to the more electropositive value, and shift anodic curve to the noble side as can be seen in Fig. 2. As $H_2O_2$ is a strong oxidizing agent, in its initial impact it thickens the oxide layer and increases cathodic current [41]. In contrast, when 10% $H_2O_2$ was applied, the potential and current density increase rapidly. This could be due to defects which are created on the oxide layer by the presence of peroxide in the SSE [41]. Even for the 0.1% $H_2O_2$, it is known that the observations are attributed only to a short period of time which $H_2O_2$ inclusion was exposed to $Ti_6Al_7Nb$. On the previous study

where $H_2O_2$ was exposed to Ti alloy, it was realised that it becomes worst as time goes on. On the other SSE modification, it was observed that maximum rapid corrosion occurs under plaque conditions (SSE modified to pH 3.0 by $H_2SO_4$). That is evidenced by quazi-broken oxide layer and a higher current density as can be seen in Fig. 2.

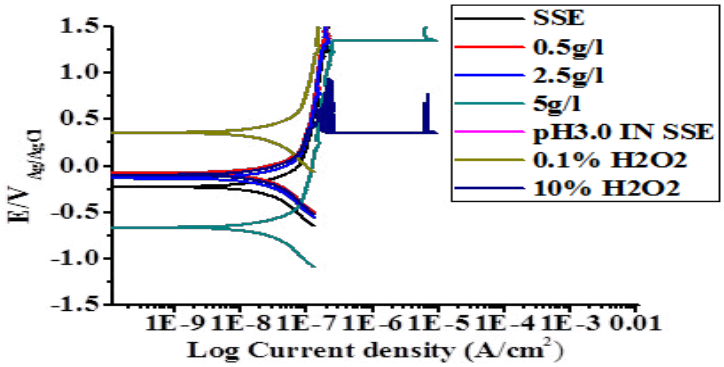


**Fig. 2:** PDP curves for $Ti_6Al_7Nb$ in different SSE conditions: Pure SSE, 0.1% $H_2O_2$, 0.5g/l NaF, 2.5gl NaF, 5g/l NaF and pH 3.0 in pure SSE (plaque condition).

PDP observations were furthermore corroborated by EIS Nyquist diagrams shown in Fig. 3. On a deeper analysis of the diagrams, it can be seen that the semicircles became more compressed when fluoride concentration increases and under severe plaque condition in SSE. This is the exact view that was observed in previous studies [17], and it is attributed to the acidified conditions which became involved therein. In Fig. 4, a higher impedance values were noted at low frequency for pure SSE and 0.1% $H_2O_2$. This once again proves the negative impact of higher fluoride concentration on $Ti_6Al_7Nb$. Higher fluoride concentration has been reported to lower corrosion resistance of implants alloys [42], and the findings herein are consistent with the previous studies. Most importantly, for engaged $Ti_6Al_7Nb$ from novel fabrication method (MIM), the fluoride content of about 5 g/l noticed to be critical. In Fig. 5, a constant phase angle curve can be seen at a low-frequency range in Fig. 5 (i), and that shows an intact passive layer which is anticipated to alloys which are used for implants [43, 44]. For this study in particular, the intact oxide layer underneath obviously porous layer ($TiO_2$) is $Nb_2O_5$, and it is shown in Fig. 6. However, as other conditions are introduced, the phase angles started to decline within the intermediate frequency range, and that is attributed to the dissolution of oxide layers [39].

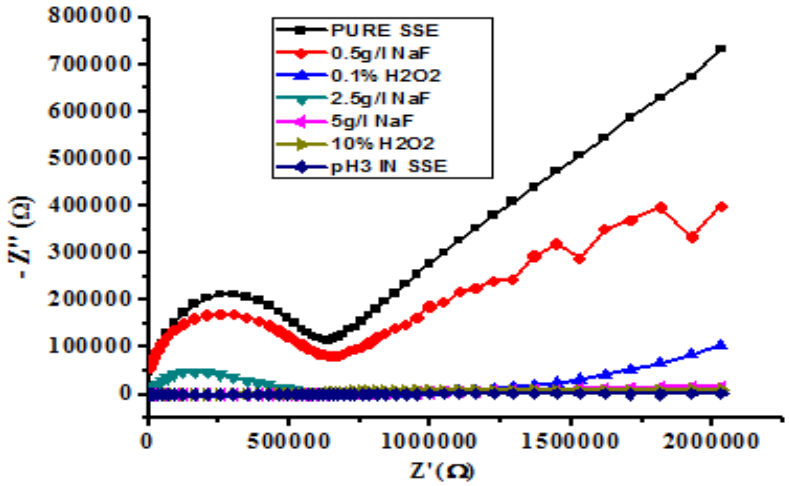


**Fig. 3:** EIS Nyquist diagrams for $Ti_6Al_7Nb$ in different SSE conditions : Pure SSE, 0.1% $H_2O_2$, 0.5g/l NaF, 2.5gl NaF, 5gl NaF and pH 3.0 in pure SSE (plaque condition).

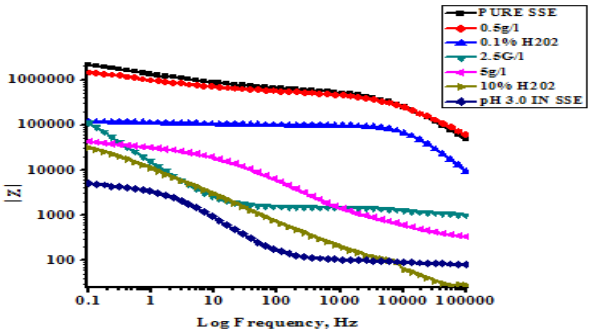


**Fig. 4:** EIS bode impedance plots (|Z|)for $Ti_6Al_7Nb$ in different SSE conditions : Pure SSE, 0.1% $H_2O_2$, 0.5g/l NaF, 2.5gl NaF, 5g/l NaF and pH 3.0 in pure SSE (plaque condition).

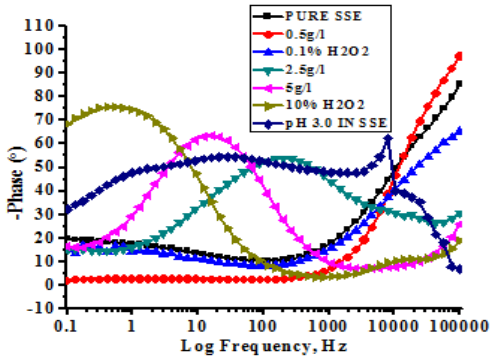


**Fig. 5:** EIS bode phase plots (°) for $Ti_6Al_7Nb$ in different SSE conditions: Pure SSE, 0.1% $H_2O_2$, 0.5g/l NaF, 2.5gl NaF, 5gl NaF, and pH 3.0 in pure SSE (plaque condition).

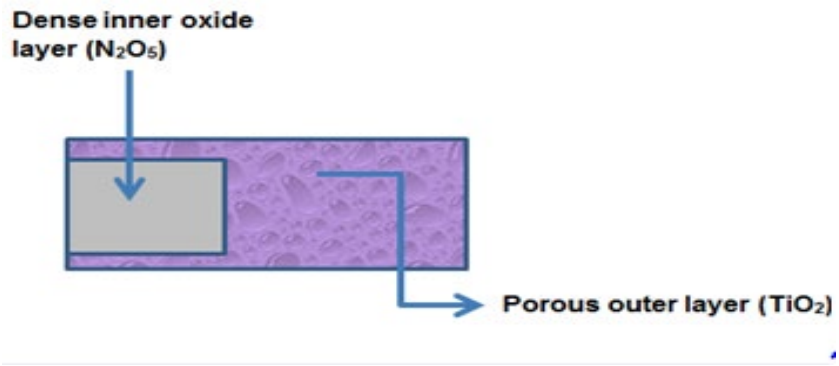


**Fig. 6:** Two layers forming on $Ti_6Al_7Nb$ under exposure to electrolytes

**Surface morphologies:** Fig. 7(a) to (g) show surface morphologies of $Ti_6Al_7Nb$ alloy when exposed to aforementioned electrolytes engaged in this study. Vividly, intact oxide layer can be seen when $Ti_6Al_7Nb$ alloy exposed to pure SSE. The morphology is composed of black and white parts as can be seen in Fig. 7a. The observation revealed alloying elements (Al and Nb) to the titanium, and this shows negligible occurrence of the degradation [45]. On 0.5 g/l NaF and 0.1% $H_2O_2$ usage as electrolytes, a uniform corrosion oxide products can be seen all over the surfaces (Fig 7(b) and (c)), and that shows mild corrosion reactions on the surface of $Ti_6Al_7Nb$ from the engaged electrolytes [46].

In opposite, when the alloy was subjected to further fluoride concentrations (2.5 and 5 g/l), aggressive surface degradation occurred on the surfaces as can be seen in Fig. 7 (d) and (e). Most notably, when the peroxide concentration was increased to 10% and under plaque conditions, aggressive surface degradation became apparent as can be seen in Fig. 7(f) and (g). All these are in agreement with previous analysis and some reported work that higher fluoride concentrations, the existence of peroxide and plaque conditions are toxic to the alloys surfaces used for implants [47], and $Ti_6Al_7Nb$ fabricated by MIM is no exception as well.

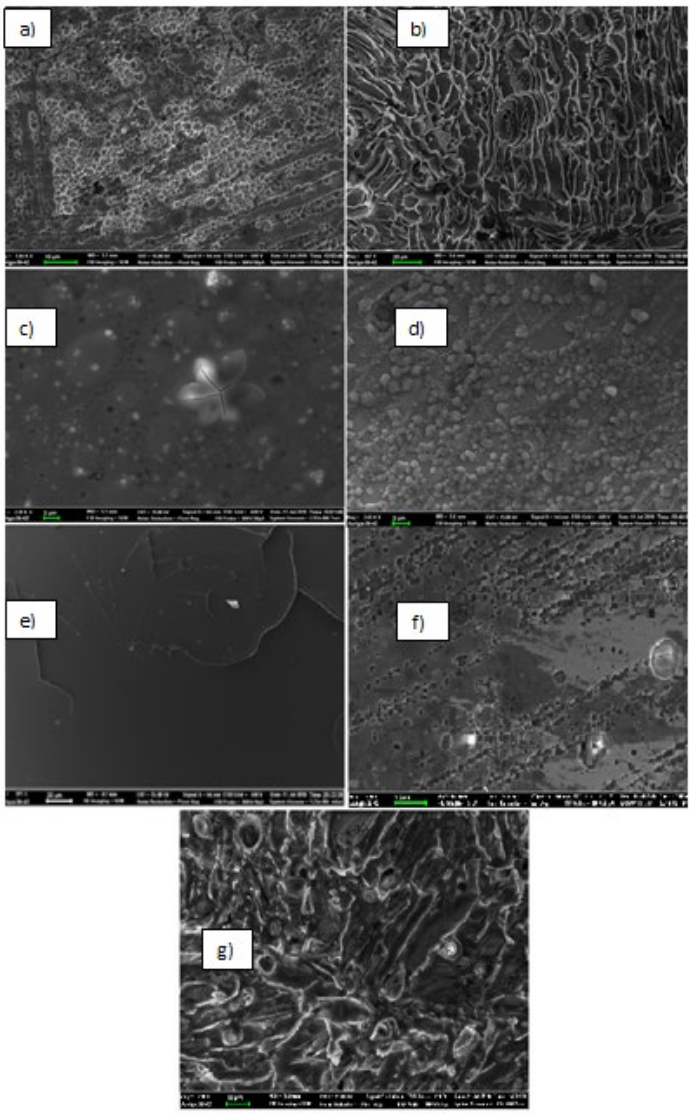


**Fig. 7:** SEM surface morphologies for $Ti_6Al_7Nb$ under dynamic SSE Two layers:
a) Pure SSE ,b) 0.5 g/l NaF, c) 0.1% $H_2O_2$, d) 2.5 g/l, e) 5 g/l, f) 10% $H_2O_2$, g) SSE at pH 3.0.

## Conclusions

Corrosion behavior of a $Ti_6Al_7Nb$ alloy, when is used as a dental implant, has been characterized in this study. From various dental application exposure, the following conclusions were drawn:

Excellent passive layer forms when $Ti_6Al_7Nb$ is exposed to pure simulating saliva electrolyte (SSE).

The increase of the fluoride concentration increases corrosion potential and corrosion kinetics, and the critical fluoride concentration was 5g/l.

Peroxide at smaller concentration causes corrosion potential to shift to the electropositive value, while the higher concentration lowers stability of the anodic passive layer forms on $Ti_6Al_7Nb$.

A simulated severe plaque formation (SSE lowered to pH 3.0) causes the most accelerated corrosion rate on $Ti_6Al_7Nb$ alloy.

Electrochemical impedance spectroscopy (EIS) measurements revealed a capacitive behavior with formation of two oxides layers (porous oxide and dense-compact oxide layer). Furthermore, high phase angle and impedance were noted at low and intermediate frequencies for pure SSE, but opposite occurrences were observed under dynamic modified SSE.

## References


1. A. Krząkała, K. Służalska, G. Dercz, A. Maciej, A. Kazek, J. Szade, A.M. Osyczka Characterisation of bioactive films on Ti–6Al–4V alloy Electrochimica Acta., 104 (2013), pp. 425-438

2. N. Ali, M. A. Fulazzaky, M. S. Mustapa, M. I. Ghazali, M. Ridha, T. Sujitno Assessment of fatigue and corrosion fatigue behaviours of the nitrogen ion implanted CpTi. International Journal of Fatigue., 61 (2014), pp. 184-190

3. M. A. Hussein, C. Suryanarayana, N. Al-Aqeeli Fabrication of nano-grained Ti–Nb–Zr biomaterials using spark plasma sintering Materials & Design., 87 (2015), pp. 693-700

4. M. Niinomi, M. Nakai, J. Hieda Development of new metallic alloys for biomedical applications Acta biomaterialia, 8 (11) (2012), pp. 3888-3903

5. A. Biesiekierski, J. Wang, M. A. H. Gepreel, C. Wen A new look at biomedical Ti-based shape memory alloys Acta biomaterialia, 8 (5) (2012)., pp. 1661-1669

6. X. Liu, P. K. Chu, C. Ding Surface modification of titanium, titanium alloys, and related materials for biomedical applications Materials Science and Engineering: R: Reports, 47 (3-4) (2004)., pp 49-121

7. A. Cremasco, W.R. Osorio, C.M. Freire, A. Garcia, R. CaramElectrochemical corrosion behavior of a Ti–35Nb alloy for medical prostheses Electrochimica Acta, 53 (14) (2008), pp. 4867-4874

8. W. Simka, M. Sowa, R.P. Socha, A. Maciej, J. Michalska Anodic oxidation of zirconium in silicate solutions Electrochimica Acta, 104 (2013), pp. 518-525

9. L. L. Rodriguez, P. A. Sundaram Corrosion behavior of plasma electrolytically oxidized gamma titanium aluminide alloy in simulated body fluid Materials chemistry and physics, 181 (2016), pp. 67-77

10. E. Vasilescu, P. Drob, D. Raducanu, I. Cinca, D. Mareci, J.C. Moreno, J.M. Rosca Effect of thermo-mechanical processing on the corrosion resistance of Ti6Al4V alloys in biofluids Corrosion Science, 51 (12) (2009), pp. 2885-2896

11. J. Fojt, L. Joska, J. Málek Corrosion behaviour of porous Ti–39Nb alloy for biomedical applications Corrosion science, 71 (2013), pp. 78-83

12. Liu, B., Shi, X. M., Xiao, G. Y., Lu, Y. P In-situ preparation of scholzite conversion coatings on titanium and Ti-6Al-4V for biomedical applications Colloids and Surfaces B: Biointerfaces, 153 (2017), pp. 291-299

13. M. F. Lopez, J. A. Jiménez, A. Gutierrez Corrosion study of surface-modified vanadium-free titanium alloys Electrochimica Acta, 48 (10) (2003), pp. 1395-1401

14. L. Thair, U. K. Mudali, N. Bhuvaneswaran, K. G. M. Nair, R. Asokamani, B. Raj Nitrogen ion implantation and in vitro corrosion behavior of as-cast Ti–6Al–7Nb alloy Corrosion Science, 44 (11) (2002), pp. 2439-2457

15. Y. S. Sun, J. F. Liu, C. P. Wu, H.H. Huang Nanoporous surface topography enhances bone cell differentiation on Ti–6Al–7Nb alloy in bone implant applications Journal of Alloys and Compounds, 643 (2015), pp. S124-S132

16. E. Chlebus, B. Kuźnicka, T. Kurzynowski, B. Dybała Microstructure and mechanical behaviour of Ti—6Al—7Nb alloy produced by selective laser melting Materials Characterization, 62 (5) (2011), pp. 488-495

17. Z. B. Wang, H. X. Hu, Y. G. Zheng, W. Ke, Y. X. Qiao Comparison of the corrosion behavior of pure titanium and its alloys in fluoride-containing sulfuric acid Corrosion Science, 103 (2016), pp.50-65

18. T.R. Rautray, R. Narayanan, K.H. Kim Ion implantation of titanium based biomaterials Progress in Materials Science, 56 (8) (2011), pp. 1137-1177

19. S. Zinelis, O. Annousaki, M. Makou, T. Eliades Metallurgical characterization of orthodontic brackets produced by metal injection molding (MIM) The Angle Orthodontist, 75 (6) (2005), pp.1024-1031

20. M. Niinomi Recent research and development in titanium alloys for biomedical applications and healthcare goods Science and technology of advanced Materials, 4 (5) (2003), pp. 445

21. M. V. Popa, E. Vasilescu, P. Drob, M. Anghel, C. Vasilescu, I. Mirza-Rosca, A.S. Lopez Anodic passivity of some titanium base alloys in aggressive environments Materials and Corrosion, 53 (1) (2002), pp. 51-55

22. J. C. Moreno, E. Vasilescu, P. Drob, P. Osiceanu, C. Vasilescu, S. I. Drob, M. Popa Surface and electrochemical characterization of a new ternary titanium based alloy behaviour in electrolytes of varying pH Corrosion Science, 77 (2013), pp.52-63

23. I. Golvano, I. García, A. Conde, W. Tato, A. Aginagalde Influence of fluoride content and pH on corrosion and tribocorrosion behaviour of Ti13Nb13Zr alloy in oral environment Journal of the mechanical behavior of biomedical materials, 49 (2015), 186-196

24. M. Nakagawa, S. Matsuya, K. Udoh Effects of fluoride and dissolved oxygen concentrations on the corrosion behavior of pure titanium and titanium alloys Dental materials journal, 21 (2) (2002), pp. 83-92

25. M. Nakagawa, S. Matsuya, T. Shiraishi, M. Ohta Effect of fluoride concentration and pH on corrosion behavior of titanium for dental use Journal of dental research, 78 (9) (1999), pp. 1568-1572

26. P. F. Santos, M. Niinomi, H. Liu, K. Cho, M. Nakai, Y. Itoh, M. Ikeda Fabrication of low-cost beta-type Ti–Mn alloys for biomedical applications by metal injection molding process and their mechanical properties Journal of the mechanical behavior of biomedical materials, 59 (2016), pp. 497-507

27. D. Zhao, K. Chang, T. Ebel, M. Qian, R. Willumeit, M. Yan, F. Pyczak Microstructure and mechanical behavior of metal injection molded Ti–Nb binary alloys as biomedical material Journal of the mechanical behavior of biomedical materials, 28 (2013), pp. 171-182

28. J. Banhart Manufacture, characterisation and application of cellular metals and metal foams Progress in materials science, 46 (6) (2001), pp. 559-632

29. E. Nyberg, M. Miller, K. Simmons, K. S. Weil Microstructure and mechanical properties of titanium components fabricated by a new powder injection molding technique Materials Science and Engineering: C, 25 (3) (2005), pp,336-342

30. O. M. Ferri, T. Ebel, R. Bormann Influence of surface quality and porosity on fatigue behaviour of Ti–6Al–4V components processed by MIM Materials Science and Engineering: A, 527 (7-8) (2010), pp. 1800-1805

31. L. Bolzoni, P. G. Esteban, E. M. Ruiz-Navas, E. Gordo Mechanical behaviour of pressed and sintered titanium alloys obtained from prealloyed and blended elemental powders Journal of the mechanical behavior of biomedical materials, 14 (2012), pp.29-38

32. Kafkas, F., Ebel, T. Metallurgical and mechanical properties of Ti–24Nb–4Zr–8Sn alloy fabricated by metal injection molding Journal of Alloys and Compounds, 617 (2014), pp. 359-366

33. G. Thavanayagam, K. L. Pickering, J. E. Swan, P. Cao Analysis of rheological behaviour of titanium feedstocks formulated with a water-soluble binder system for powder injection moulding Powder Technology, 269 (2015), pp. 227-232

34. P. F. Santos, M. Niinomi, K. Cho, M. Nakai, H. Liu, N. Ohtsu, T. Narushima Microstructures, mechanical properties and cytotoxicity of low cost beta Ti–Mn alloys for biomedical applications

Acta biomaterialia, 26 (2015), pp. 366-376

35. S. Ehtemam-Haghighi, Y. Liu, G. Cao, L. C. Zhang Phase transition, microstructural evolution and mechanical properties of Ti-Nb-Fe alloys induced by Fe addition Materials & Design, 97 (2016), pp. 279-286

36. L. Bolzoni, E. M. Ruiz-Navas, E. Gordo Evaluation of the mechanical properties of powder metallurgy Ti-6Al-7Nb alloy Journal of the mechanical behavior of biomedical materials, 67 (2017), pp. 110-116

37. G. Mabilleau, S. Bourdon, Joly-Guillou, M. L., Filmon, R., Baslé, M. F., Chappard, D. Influence of fluoride, hydrogen peroxide and lactic acid on the corrosion resistance of commercially pure titanium

Acta biomaterialia, 2 (1) (2006), pp. 121-129

38. N. Rinčić, I. Baučić, S. Miko, M. Papić, E. Prohić Corrosion behaviour of the Co-Cr-Mo dental alloy in solutions of different composition and different pH values Collegium antropologicum, 27 (2) (2003), pp. 99-106

39. Fattah-alhosseini, A., Ansari, A. R., Mazaheri, Y., Karimi, M Electrochemical Behavior Assessment of Micro-and Nano-Grained Commercial Pure Titanium in H 2 SO 4 Solutions Journal of Materials Engineering and Performance, 26 (2) (2017), pp. 611-620

40. A. Revathi, A. D. Borrás, A. I. Muñoz, C. Richard, G. Manivasagam Degradation mechanisms and future challenges of titanium and its alloys for dental implant applications in oral environment

Materials Science and Engineering: C, 76 (2017), pp. 1354-1368

41. Y. Zhang, O. Addison, F. Yu, B. C. R. Troconis, J. R. Scully, A. J. Davenport Time-dependent Enhanced Corrosion of Ti6Al4V in the Presence of H 2O2 and Albumin. Scientific reports, 8 (1) (2018), pp. 3185

42. C. Pirvu, Demetrescu, I., Drob, P., Vasilescu, E., Ivanescu, S., Mindroiu, M., Drob, S. I. Corrosion behaviour of a new Ti-6Al-2Nb-1Ta alloy in various solutions Materials and Corrosion, 62 (10) (2011), pp. 948-955

43. A. Meroufel, C. Deslouis, S. TouzainElectrochemical and anticorrosion performances of zinc-rich and polyaniline powder coatings Electrochimica Acta, 53 (5) (2008), pp. 2331-2338

44. S. Kumar, T. S. Narayanan, S. G. S. Raman, S. K. Seshadri Thermal oxidation of CP-Ti: Evaluation of characteristics and corrosion resistance as a function of treatment time Materials Science and Engineering: C, 29 (6) (2009), pp. 1942-1949

45. Y. J. Bai, Y. B. Wang, Y. Cheng, F. Deng, Y. F. Zheng , S. C. Wei Comparative study on the corrosion behavior of Ti–Nb and TMA alloys for dental application in various artificial solutions Materials Science and Engineering: C, 31 (3) (2011), pp. 702-711

46. Y. Bai, Y. L. Hao, S. J. Li, Y. Q. Hao, R. Yang, F. Prima Corrosion behavior of biomedical Ti–24Nb–4Zr–8Sn alloy in different simulated body solutions Materials Science and Engineering: C, 33 (4) (2013), pp. 2159-2167

47. L. Reclaru, J. M. Meyer Effects of fluorides on titanium and other dental alloys in dentistry Biomaterials, 19 (1-3) (1998), pp. 85-92